

Fourier analysis of luminosity-dependent galaxy clustering

Will J. Percival¹, Licia Verde^{2,3}, John A. Peacock¹

¹*Institute for Astronomy, University of Edinburgh, Royal Observatory, Blackford Hill, Edinburgh EH9 3HJ, UK*

²*Dept. Astrophysical sciences, Princeton University, Ivy Lane, Princeton, NJ 08540, USA*

³*Department of Physics & Astronomy, University of Pennsylvania, 209 South 33rd Street Philadelphia, PA 19104, USA*

Submitted for publication in MNRAS

ABSTRACT

We extend the Fourier transform based method for the analysis of galaxy redshift surveys of Feldman, Kaiser & Peacock (1994: FKP) to model luminosity-dependent clustering. In a magnitude limited survey, galaxies at high redshift are more luminous on average than galaxies at low redshift. Galaxy clustering is observed to increase with luminosity, so the inferred density field is effectively multiplied by an increasing function of radius. This has the potential to distort the shape of the recovered power spectrum. In this paper we present an extension of the FKP analysis method to incorporate this effect, and present revised optimal weights to maximize the precision of such an analysis. The method is tested and its accuracy assessed using mock catalogues of the 2-degree field galaxy redshift survey (2dFGRS). We also show that the systematic effect caused by ignoring luminosity-dependent bias was negligible for the initial analysis of the 2dFGRS of Percival et al. (2001). However, future surveys, sensitive to larger scales, or covering a wider range of galaxy luminosities will benefit from this refined method.

Key words: cosmology: observations – large-scale structure of Universe – cosmological parameters – surveys

1 INTRODUCTION

The shape of the matter power spectrum as traced by large-scale structure is one of the cornerstones of modern cosmology. The shape is dependent on the primordial fluctuations, on the total matter density Ω_m through $\Omega_m h$ which controls the matter-radiation horizon scale, and through the fraction of matter in baryons Ω_b/Ω_m . Although these parameter combinations are nearly degenerate, preliminary results from the 2-degree field galaxy redshift survey (2dFGRS) contained sufficient signal to weakly break this degeneracy (Percival et al. 2001: P01). The complete 2dFGRS, the Sloan Digital Sky Survey (SDSS; York et al. 2000) and forthcoming high-redshift surveys will refine these measures of the cosmological matter content from large-scale structure observations.

High-quality measurements of the cosmic microwave background (CMB) power spectrum (e.g. Bennett et al. 2003; Hinshaw et al. 2003) have brought about a new era of high-precision cosmology, in which the analysis of large-scale structure (LSS) data assumes even greater importance. Many of the degeneracies between cosmological parameters intrinsic to CMB data are broken by the addition of constraints from LSS data (e.g. Efstathiou et al. 2002; Percival et al. 2002; Spergel et al. 2003; Verde et al. 2003). Thus, the scientific potential of both data sets can be greatly enhanced through combination. However, the physics and instrumental effects involved in the interpretation of LSS data are more complicated and less well understood than for the CMB data. To use LSS

reliably in the context of high-precision cosmology, it is therefore important to consider the survey analysis method and any possible systematic problems in detail.

There are a number of difficulties and potential systematic effects associated with recovering the shape of the matter power spectrum from that of the galaxies. Distances to galaxies are derived from redshifts, and peculiar velocities induce systematic distortions in the recovered power. Although this effect is important and potentially carries cosmological information (e.g. Peacock et al. 2001; Hawkins et al. 2003; see Hamilton 1998 for a review), we will not address it here, but we will consider a more subtle effect. Galaxies are biased tracers of the matter distribution: the relation between the galaxy and mass density fields is probably both non-linear and stochastic to some extent (e.g. Dekel & Lahav 1999), so that the power spectra of galaxies and mass differ in general. If we define scale-dependent bias via

$$P_g(k) = b^2(k)P_m(k), \quad (1)$$

where subscripts m and g denote matter and galaxies respectively, there is no guarantee that $b(k)$ will be a constant. The best we can hope for is that there will be a ‘linear response’ limit, in which $b(k)$ tends to a constant b_{lin} on large scales. Although it is easy to invent artificial models in which this is not true, the concept of linear bias does hold for many bias models – and in particular for the most detailed attempts to include all the physics of galaxy formation (e.g.

arXiv:astro-ph/0306511v2 25 Sep 2003

Benson et al. 2000). Such simulations can also give a realistic idea of the scales on which the linear-bias assumption breaks down, and we assume for the purposes of this paper that linear bias is true (or that small deviations from scale-independence can be corrected for). Nevertheless, even in the linear-bias limit, bias can complicate the analysis of LSS data, because the value of b_{lin} will be different for different classes of galaxy. The purpose of this paper is to investigate the extent to which this can affect the recovered power spectrum shape.

The fact that galaxies selected in different ways have different clustering properties has been known for some time (e.g. Davis & Geller 1976; Peacock & Dodds 1994; Seaborn et al. 1999). For the 2dFGRS galaxies, although the average bias is close to unity (Lahav et al. 2002; Verde et al. 2002), the bias is dependent on galaxy luminosity (Norberg et al. 2001; 2002; Zehavi et al. 2002 find a very similar dependence for SDSS galaxies), with

$$\left\langle \frac{b(L)}{b(L_*)} \right\rangle = 0.85 + 0.15 \frac{L}{L_*}, \quad (2)$$

where the bias $b(L)$ is assumed to be a simple function of galaxy luminosity and L_* is defined such that $M_{b_j} - 5 \log_{10} h = -19.7$ (Norberg et al. 2001).

In a magnitude limited survey, galaxies of different luminosities are probed at different radii: at high redshift, galaxies more luminous than average (and with lower number density) dominate the sample, while at low redshift galaxies less luminous than average (and with higher number density) dominate. As a consequence, the power spectrum at large scales is measured preferentially from galaxies more luminous than average, and on small scales from galaxies less luminous than average. Without correction, luminosity-dependent bias would therefore distort the shape of the recovered galaxy power spectrum from that of the matter power spectrum (see Tegmark et al. 2003).

In this paper we consider how best to estimate the shape of the underlying matter power spectrum given a sample of galaxies that have a clustering amplitude dependent on galaxy properties. Specifically, in Section 2 we consider a set of galaxies with a simple luminosity-dependent bias such that, on the scales of interest $P_g(k) = b^2(L)P_m(k)$. For generality, the expected bias need not be simply a function of luminosity; all that is required is that the bias can be predicted from some combination of the properties of each galaxy. The results of this paper are therefore relevant to more general problems where we have a mixed set of galaxies tracing the same density field. For instance the method would be applicable to type-dependent clustering or a survey covering a large redshift range where the linear evolution of the matter power spectrum and evolution in the bias of the objects selected were important.

Previous studies have already extended the calculation of optimal weights presented by FKP. Hamilton (1997) considered the effect of the window function which the FKP method assumes to be negligible. More recently, Yamamoto (2003) attempted to derive optimal weights including the effect of both redshift-space distortions and the light-cone effect, which, as we will illustrate later, has a similar net effect as luminosity dependent bias. In this paper, the work of FKP is extended in a different context to the work of Yamamoto (2003), and we consider the systematic effect of luminosity-dependent bias on the recovered power in addition to providing optimal weights. Interestingly, our derived optimal weights, following an independent calculation, differ from those of Yamamoto (2003) and a comparison is given in Section 5.

The layout of this paper is as follows. First, in Section 2.1 we present a generalization of the power spectrum analysis method in-

roduced by Feldman, Kaiser & Peacock (1994: FKP), extended to correct for galaxy luminosity dependent bias. We then follow the FKP derivation leading to revised optimal weights in Section 2.3, in the limit of a large survey volume. The method and weights are tested in Section 3 using simple mock catalogues with a window function similar to that of the 2dFGRS, and the relevance for the analysis of P01 is considered in Section 4. We conclude in Section 5.

2 ANALYSIS OF A MIXED LUMINOSITY SAMPLE

In this Section we extend the method of FKP to cover a sample of galaxies with different large-scale biases. In order to make the description transparent, we adopt the notation of FKP, and refer extensively to this paper. In particular, we adopt the Fourier transform convention of FKP, equivalent to that of Peebles (1980) with $V = 1$.

2.1 Method

Let us consider a set of galaxies of luminosity L forming a Poisson sampling of a linearly biased density field

$$1 + \delta_g(\mathbf{r}) = 1 + b(\mathbf{r}, L)\delta(\mathbf{r}). \quad (3)$$

Here $b(\mathbf{r}, L)$ is the linear bias of galaxies of luminosity L at position \mathbf{r} . We have generalized the idea of bias being a function of L only to allow for e.g. slow evolution of $b(L)$ within the survey volume. The probability that volume element δV contains a galaxy of luminosity L is given by

$$\text{Prob}(\delta V, L) = \delta V \bar{n}(\mathbf{r}, L)[1 + b(\mathbf{r}, L)\delta(\mathbf{r})], \quad (4)$$

where $\bar{n}(\mathbf{r}, L)$ is the mean expected number density of galaxies at \mathbf{r} with luminosity L . The power spectrum and correlation function form a Fourier pair with $\xi(\mathbf{r}) = \xi(r) = \langle \delta(\mathbf{r}')\delta(\mathbf{r}'+\mathbf{r}) \rangle$, and

$$P(\mathbf{k}) = P(k) = \int d^3r \xi(\mathbf{r}) e^{i\mathbf{k}\cdot\mathbf{r}}. \quad (5)$$

Here and hereafter $P(k)$ denotes the power spectrum of the underlying matter fluctuation field δ . If, rather than considering the bias of each galaxy, we had instead considered the ratio of the bias to that of a particular galaxy type, then we simply have to redefine $P(k)$ as the power spectrum of that galaxy type. Replacing $b(\mathbf{r}, L)$ by $b(\mathbf{r}, L)/b(\mathbf{r}, L_*)$ would mean that $P(k)$ would have to be redefined as the power spectrum of L_* galaxies so, for the 2dFGRS galaxies, we could use Eq. 2 to recover the power spectrum of L_* galaxies.

Following the FKP approach, we also consider a synthetic catalogue with the same radial and angular sampling (selection function), and luminosity distribution as the galaxy catalogue but with no correlations. This synthetic catalogue will be used (Eq. 6) to convert from a galaxy density field to a galaxy overdensity field. We will multiply objects in both the galaxy and synthetic catalogue by $w(\mathbf{r}, L)/b(\mathbf{r}, L)$ – here the split distinguishes the bias correction and additional weighting needed to optimize the precision of the power estimate. For clarity in the following text, we only use the “weight” to refer to $w(\mathbf{r}, L)$, not $w(\mathbf{r}, L)/b(\mathbf{r}, L)$.

The weighted galaxy fluctuation field is defined as

$$F(\mathbf{r}) \equiv \frac{1}{N} \int dL \frac{w(\mathbf{r}, L)}{b(\mathbf{r}, L)} [n_g(\mathbf{r}, L) - \alpha n_s(\mathbf{r}, L)] \quad (6)$$

where $n_g(\mathbf{r}, L) = \sum_j \delta(\mathbf{r} - \mathbf{r}_j) \delta(L - L_j)$, with \mathbf{r}_j being the location of the j th galaxy of luminosity L_j , and $n_s(\mathbf{r}, L)$ is defined similarly for the synthetic catalogue. Here α is a constant that matches the two catalogues (see Section 2.4), and N is a normalization constant defined by

$$N = \left\{ \int d^3r \left[\int dL \bar{n}(\mathbf{r}, L) w(\mathbf{r}, L) \right]^2 \right\}^{1/2}. \quad (7)$$

Following appendix A of FKP, the two-point functions of n_g, n_s are

$$\begin{aligned} \langle n_g(\mathbf{r}, L) n_g(\mathbf{r}', L') \rangle = & \\ & \bar{n}(\mathbf{r}, L) \bar{n}(\mathbf{r}', L') [1 + b(\mathbf{r}, L) b(\mathbf{r}', L') \xi(\mathbf{r} - \mathbf{r}')] \\ & + \bar{n}(\mathbf{r}, L) \delta(\mathbf{r} - \mathbf{r}') \delta(L - L'), \end{aligned} \quad (8)$$

$$\begin{aligned} \langle n_s(\mathbf{r}, L) n_s(\mathbf{r}', L') \rangle = & \alpha^{-2} \bar{n}(\mathbf{r}, L) \bar{n}(\mathbf{r}', L') \\ & + \alpha^{-1} \bar{n}(\mathbf{r}, L) \delta(\mathbf{r} - \mathbf{r}') \delta(L - L'), \end{aligned} \quad (9)$$

$$\langle n_g(\mathbf{r}, L) n_s(\mathbf{r}', L') \rangle = \alpha^{-1} \bar{n}(\mathbf{r}, L) \bar{n}(\mathbf{r}', L'), \quad (10)$$

where we have explicitly included the bias caused by the different galaxy luminosities. The expected value $\langle F(\mathbf{r}) F(\mathbf{r}') \rangle$ is therefore given by

$$\langle F(\mathbf{r}) F(\mathbf{r}') \rangle = G(\mathbf{r}) G(\mathbf{r}') \xi(\mathbf{r} - \mathbf{r}') + \xi_{\text{shot}}(\mathbf{r}, \mathbf{r}'), \quad (11)$$

where

$$G(\mathbf{r}) = \frac{1}{N} \int dL \bar{n}(\mathbf{r}, L) w(\mathbf{r}, L), \quad (12)$$

and

$$\xi_{\text{shot}}(\mathbf{r}, \mathbf{r}') = \frac{1 + \alpha}{N^2} \int dL \bar{n}(\mathbf{r}, L) \frac{w^2(\mathbf{r}, L)}{b^2(\mathbf{r}, L)} \delta(\mathbf{r} - \mathbf{r}'). \quad (13)$$

The first term in Eq. 11 corresponds to the multiplication of the correlation function by the window. The second is the shot noise term. Switching to Fourier space we have, as in FKP, that

$$\langle |F(\mathbf{k})|^2 \rangle = \int \frac{d^3k'}{(2\pi)^3} P(\mathbf{k}') |G(\mathbf{k} - \mathbf{k}')|^2 + P_{\text{shot}}. \quad (14)$$

The multiplication in real space (the first term in Eq. 11) has become a convolution in Fourier space (the first term in Eq. 14), but now

$$G(\mathbf{k}) = \frac{1}{N} \int d^3r \int dL \bar{n}(\mathbf{r}, L) w(\mathbf{r}, L) e^{i\mathbf{k} \cdot \mathbf{r}}, \quad (15)$$

and

$$P_{\text{shot}} = \frac{1 + \alpha}{N^2} \int d^3r \int dL \bar{n}(\mathbf{r}, L) \frac{w^2(\mathbf{r}, L)}{b^2(\mathbf{r}, L)}. \quad (16)$$

Ignoring the bias changes between galaxies with different luminosities reduces $G(\mathbf{k})$ and P_{shot} to the FKP expressions.

The factorization of the multiplicative factor in Eq. 6 is now clear: although we multiply by $w(\mathbf{r}, L)/b(\mathbf{r}, L)$, the window function shape (Eq. 15) and normalization (Eq. 7) are only dependent on the weights $w(\mathbf{r}, L)$: the additional $1/b(\mathbf{r}, L)$ factor simply corrects the measured galaxy fluctuations to an estimate of the matter fluctuations, and does not affect the window.

Our estimator of $P(\mathbf{k})$ convolved with the window function is given by $\hat{P}(\mathbf{k}) = |F(\mathbf{k})|^2 - P_{\text{shot}}$. Averaging over a shell in k -space, gives our final estimator of the convolved power $P(k)$, $\hat{P}(k)$,

$$\hat{P}(k) \equiv \frac{1}{V_k} \int_{V_k} d^3k' \hat{P}(\mathbf{k}'), \quad (17)$$

where V_k is the volume of the shell. Ignoring redshift-space distortions, $\hat{P}(k)$ is the true power spectrum convolved with a spherically-averaged window, which can be computed by spherically averaging $|G(\mathbf{k})|^2$, with $G(\mathbf{k})$ given by Eq. 15. Redshift-space distortions mean that the interpretation of Eq. 17 is actually more complicated, and $\hat{P}(k)$ depends on the full survey window. In the spirit of generalizing FKP, such effects are not included here; a separate study of this issue would nevertheless be of interest.

We can now contrast the FKP procedure with the exact analysis of luminosity-dependent clustering, as expressed in Eqns. 14 – 16. FKP used luminosity-independent weights, equivalent to $w(\mathbf{r}, L) = b(\mathbf{r}, L) w_{\text{FKP}}(\mathbf{r})$ in our current notation. The resulting density fluctuation field (Eq. 6) differs from the corresponding quantity in FKP, because the normalization factor, N , contains $w(\mathbf{r}, L)$. We therefore have $F_{\text{FKP}}(\mathbf{r}) = b_{\text{eff}} F(\mathbf{r})$, where

$$b_{\text{eff}}^2 = \frac{\int d^3r \left[\int dL \bar{n}(\mathbf{r}, L) b(\mathbf{r}, L) w_{\text{FKP}}(\mathbf{r}) \right]^2}{\int d^3r \left[\int dL \bar{n}(\mathbf{r}, L) w_{\text{FKP}}(\mathbf{r}) \right]^2} \quad (18)$$

This effective bias is potentially more serious than just a shift in the overall normalization, since $w_{\text{FKP}} = 1/[1 + \bar{n}P(k)]$ is a function of wavenumber: a different $F(\mathbf{r})$ is to be transformed for each k value. This means that b_{eff} is also a function of k , and the shape of the recovered spectrum is systematically altered. However, most analyses (including P01) have not taken the FKP mantra to this extreme, and have in practice assumed a single value for $P(k)$ at all wavenumbers. Therefore, the P01 analysis is not affected by this potential difficulty.

Even so, there is a second difference between our results and FKP, which may be seen in Eq. 15. The derived power spectrum is an estimate of the true power convolved with a window function $|G(k)|^2$, and the correct form for this window differs from the corresponding function in the FKP analysis. As shown in P01, this convolution significantly changes the shape of the recovered power spectrum, and so we are led to ask whether the change in the window is important; we show below in Section 3.4 that it is not.

Finally, although we are thus able to identify potential systematic errors that can arise from application of the FKP procedure to luminosity-dependent clustering, this does not address the issue of optimality. In fact, the original FKP weight is not optimal in general – nor is the simple bias-corrected multiple of it. A derivation of the correct optimal weight (in the usual limit of a narrow k -space window) is presented in Section 2.3.

2.2 Statistical fluctuations in the convolved 3D power

We now proceed to analyse the error in our power estimator, as in FKP section 2.2. We assume that the Fourier components $F(\mathbf{k})$ are Gaussian-distributed, so the variance in our estimate of the convolved power $\langle \delta \hat{P}(\mathbf{k}) \delta \hat{P}(\mathbf{k}') \rangle = \langle |F(\mathbf{k}) F^*(\mathbf{k}')|^2 \rangle$ (FKP Appendix B). On the large-scales of interest this is a good approximation in the limit of a compact window function. Following the same steps as in FKP section 2.2, our estimate of the mean square fluctuations in the recovered convolved power $\langle F(\mathbf{k}) F^*(\mathbf{k} + \delta \mathbf{k}) \rangle$ is given by

$$\langle F(\mathbf{k}) F^*(\mathbf{k} + \delta \mathbf{k}) \rangle \simeq P(\mathbf{k}) Q(\delta \mathbf{k}) + S(\delta \mathbf{k}), \quad (19)$$

where

$$Q(\mathbf{k}) = \frac{1}{N^2} \int d^3 r \left[\int dL \bar{n}(\mathbf{r}, L) w(\mathbf{r}, L) \right]^2 e^{i\mathbf{k}\cdot\mathbf{r}}, \quad (20)$$

and

$$S(\mathbf{k}) = \frac{1+\alpha}{N^2} \int d^3 r \int dL \bar{n}(\mathbf{r}, L) \frac{w^2(\mathbf{r}, L)}{b^2(\mathbf{r}, L)} e^{i\mathbf{k}\cdot\mathbf{r}}. \quad (21)$$

This leads to an estimate of the error in the convolved power

$$\langle \delta \hat{P}(\mathbf{k}) \delta \hat{P}(\mathbf{k}') \rangle = |P(\mathbf{k})Q(\delta\mathbf{k}) + S(\delta\mathbf{k})|^2. \quad (22)$$

2.3 Optimal Weighting

Optimal weights can now be derived for such an analysis following a direct extrapolation of FKP section 2.3.

We assume that the window function is compact in k -space compared with the scales of interest; this will be discussed in more detail in Section 5. The mean square fluctuation in our estimate of the power is

$$\sigma_P^2(k) \equiv \langle [\hat{P}(k) - P(k)]^2 \rangle \quad (23)$$

$$= \frac{1}{V_k^2} \int_{V_k} d^3 k \int_{V_k} d^3 k' \langle \delta \hat{P}(\mathbf{k}) \delta \hat{P}(\mathbf{k}') \rangle. \quad (24)$$

If the shell over which we average has a width that is large compared to the effective width of $Q(\mathbf{k})$, but small compared with the variation in $P(k)$, then this double integral reduces to

$$\sigma_P^2(k) \simeq \frac{1}{V_k} \int d^3 k' |P(k)Q(\mathbf{k}') + S(\mathbf{k}')|^2. \quad (25)$$

Using the definitions of $Q(\mathbf{k})$ and $S(\mathbf{k})$ from Eqns. 20 & 21, and Parseval's theorem, the fractional variance in the power is

$$\frac{\sigma_P^2(k)}{P^2(k)} = \frac{(2\pi)^3}{V_k N^4} \int d^3 r \left\{ \left[\int dL \bar{n}(\mathbf{r}, L) w(\mathbf{r}, L) \right]^2 + \left[\int dL \bar{n}(\mathbf{r}, L) \frac{w^2(\mathbf{r}, L)}{b^2(\mathbf{r}, L)} \right] \frac{1}{P(k)} \right\}^2. \quad (26)$$

We wish to find $w(\mathbf{r}, L)$ that minimize Eq. 26. Without loss of generality, we consider a small variation in the weights $w(\mathbf{r}, L) \rightarrow w(\mathbf{r}, L) + \delta(L - L')\delta w'(\mathbf{r})$. To keep the equations concise, we set $w \equiv w(\mathbf{r}, L)$, $\bar{n} \equiv \bar{n}(\mathbf{r}, L)$, $b \equiv b(\mathbf{r}, L)$ and $P \equiv P(k)$. Similarly, $w' \equiv w(\mathbf{r}, L')$, $\bar{n}' \equiv \bar{n}(\mathbf{r}, L')$ and $b' \equiv b(\mathbf{r}, L')$. Requiring that $\sigma_P^2(k)$ be stationary with respect to arbitrary variations $\delta w'(\mathbf{r})$ gives that

$$\frac{\int d^3 r \left[\left(\int dL \bar{n}w \right)^2 + \left(\int dL \frac{\bar{n}w^2}{Pb^2} \right) \right] \left[\bar{n}' \left(\int dL \bar{n}w \right) + \frac{\bar{n}'w'}{Pb'^2} \right] \delta w'}{\int d^3 r \left[\left(\int dL \bar{n}w \right)^2 + \left(\int dL \frac{\bar{n}w^2}{Pb^2} \right) \right]^2} = \frac{\int d^3 r \bar{n}' \left(\int dL \bar{n}w \right) \delta w'}{\int d^3 r \left(\int dL \bar{n}w \right)^2}. \quad (27)$$

The non-trivial solution to this Equation is

$$w(\mathbf{r}, L') = \frac{b^2(\mathbf{r}, L')P(k)}{1 + \int dL \bar{n}(\mathbf{r}, L)b^2(\mathbf{r}, L)P(k)}, \quad (28)$$

which is the principal result of this paper.

This formula was found by considering initially the case of two sets of galaxies with different luminosities, so the integral is replaced by a sum over the two subsets. The resulting equations were then solved with the aid of MATHEMATICA. The form of the

2-class solution suggested a conjecture for the general solution with a countable number of sets of galaxies, and thus for a set of galaxies with a continuous distribution of luminosities. The conjecture was readily verified by direct substitution. It is straightforward to see that this reduces to the formula of FKP (their equation 2.3.4) for a sample of galaxies at a single luminosity.

Eq. 28 shows that $w(\mathbf{r}, L)$ depends not only on the expected bias of galaxies of that luminosity $b(\mathbf{r}, L)$, but additionally on the bias of galaxies of all luminosities at this location through $\int dL \bar{n}(\mathbf{r}, L)b^2(\mathbf{r}, L)$. This follows because the balance between shot noise and cosmic variance, which is at the heart of the derivation of the optimal weights, depends on what we learn from all galaxies whatever their luminosity. It is also interesting to note that, while the contribution of galaxies to the overdensity estimate appears to be inversely proportional to their bias (the $1/b(\mathbf{r}, L)$ factor in Eq. 6), optimizing the weight actually means that the net contribution of these galaxies is increased – they contain the most signal-to-noise because of their strong clustering.

2.4 Choice of α

The value of α in Eq. 6 sets the expected number of galaxies for a particular survey. In this Section we discuss how this can be set given no information other than the survey itself.

Suppose that we had used an incorrect value of α in Eq. 6, so that this Equation became

$$F(\mathbf{r}) \equiv \frac{1}{N} \int dL \frac{w(\mathbf{r}, L)}{b(\mathbf{r}, L)} [n_g(\mathbf{r}, L) - (\alpha - \beta)n_s(\mathbf{r}, L)], \quad (29)$$

then the effect of the additional component is to introduce an additional term

$$\frac{\beta^2}{\alpha^2} \int \frac{d^3 k}{(2\pi)^3} |G(\mathbf{k})|^2 \quad (30)$$

to the right hand side of Eq. 14. Turning this argument around, we see that not knowing the true value of α is equivalent to adding a multiple of the Fourier transformed window function to our power estimate. In general, the average weighted galaxy density has to be derived from the survey itself, and it is therefore impossible to know the true offset between the number of galaxies observed and that expected. In this situation, the only sensible thing to do is to set

$$\alpha = \frac{\int d^3 r \int dL \frac{w(\mathbf{r}, L)}{b(\mathbf{r}, L)} n_g(\mathbf{r}, L)}{\int d^3 r \int dL \frac{w(\mathbf{r}, L)}{b(\mathbf{r}, L)} n_s(\mathbf{r}, L)}, \quad (31)$$

so that the average weighted overdensity is artificially set to zero. This self-normalization forces $P(0) = 0$ and results in a deficit in the estimated power equivalent to subtracting a scaled copy of the window function, centered on $k = 0$ (Peacock & Nicholson 1991). In the limit of no window, the effect of this self-normalization would be to remove a delta function located at $k = 0$ such that $P(0) = 0$. In effect, this procedure evades the possibility of noise in our estimate of large-scale power owing to the uncertainty in \bar{n} , at the expense of systematic damping of the large-scale signal (cf. the approach of Tadros & Efstathiou 1995).

2.5 A note on the convention adopted

Instead of allowing for a continuous distribution of galaxy luminosities and corresponding biases, an alternative approach would have been to consider a countable number of sets of galaxies with different luminosities. In this case, Eq. 6 would have become

$$F(\mathbf{r}) \equiv \frac{1}{N} \sum_i \frac{w(\mathbf{r}, L_i)}{b(\mathbf{r}, L_i)} [n_g(\mathbf{r}, L_i) - \alpha n_s(\mathbf{r}, L_i)] \quad (32)$$

where $n_g(\mathbf{r}, L_i) = \sum_j \delta(\mathbf{r} - \mathbf{r}_j)$ now gives the density of galaxies within subset i , the subset containing those galaxies of luminosity L_i . The analysis and derivation of optimal weights described in this paper follows exactly as for the continuous case, except that we obviously need to replace the integral over luminosity with a sum over the subsets of galaxies throughout.

3 APPLICATION TO MOCK CATALOGUES

Having introduced the necessary formalism, we now illustrate the revised FKP method using simple artificial surveys. These artificial surveys were designed to approximate the selection function and luminosity-dependent bias of the 2dFGRS galaxies analysed by P01.

3.1 Selection function

The selection function is approximately matched to the part-complete 2dFGRS survey (Colless et al. 2001) as analysed in P01. The redshift distribution used for the galaxies is given by

$$f(z) = z^{1.25} \exp \left[- \left(\frac{z}{0.13} \right)^{2.2} \right], \quad (33)$$

and limited to $0 < z < 0.25$.

This radial selection function corresponds to the angle-averaged selection function of the survey as analyzed in P01 including both the NGP, SGP and random fields. However the selection function does not exactly match that of P01 as it does not include the varying survey depth of the 2dFGRS sample (see Colless et al. 2001 for details). As we simply wish to compare and contrast our revised analysis method and the effect of not taking into consideration luminosity-dependent bias, this difference is not important. The expected number of galaxies in each catalogue was set at 140 000, although the actual number varies through Poisson sampling (see Section 3.2).

In the following analysis we use a $512 \times 512 \times 256$ grid that just covers the survey region: given the survey geometry, the rectangular nature of this grid yields roughly similar sampling, and therefore Nyquist frequencies, in each Cartesian direction.

3.2 Creating the mock catalogues

In this Section we describe how the mock galaxy catalogues, drawn from lognormal random fields, were generated (this closely follows the method described in Coles & Jones 1991). Lognormal random fields were used for convenience because they obey the physical limit $\delta(\mathbf{r}) > -1 \forall \mathbf{r}$, and approximate the present-day non-linear fluctuation field.

The underlying matter power spectrum was chosen to be a Λ CDM model calculated from the transfer function fitting formulae of Eisenstein & Hu (1999) coupled with the non-linear fitting formulae of Smith et al. (2002). The following cosmological parameter values were set: $\Omega_m = 0.3$, $\Omega_b/\Omega_m = 0.15$, $\Omega_\Lambda = 0.7$, $h = 0.7$, $n_s = 1$ (consistent with the recent WMAP results – Spergel et al. 2003). The normalization of the power spectrum (chosen to be $\sigma_8 = 1$) is unimportant for our analysis, which focuses on the relative change in the recovered power with various weighting schemes rather than the absolute value. In addition, we will

use Eq. 2 to determine bias relative to L_* galaxies rather than the absolute bias, so the power spectrum normalization chosen should correspond to that of L_* galaxies.

This power spectrum was determined on the grid described in Section 3.1. In order to avoid a sharp cut-off in the power, we introduce a smooth turn over at 0.1 times the minimum Nyquist frequency, ν_{Ny} , which cuts the input power at $0.25\nu_{Ny}$. This does not affect any of our conclusions as we are only interested in the large-scale power $k < 0.15 h \text{ Mpc}^{-1}$. The input power was inverse Fourier transformed to obtain the correlation function of the lognormal field required. The covariance of the Gaussian field, required to generate the lognormal field, is then obtained from $\xi_G(r) = \ln[1 + \xi_{LN}(r)]$, and this was converted back to the power. A Gaussian density field δ_G was then generated on the grid with this power spectrum, and the corresponding lognormal field was calculated, given by $\delta_{LN} = \exp(\delta_G - \sigma_G^2/2) - 1$, where σ_G^2 is the variance of the Gaussian density field.

The lognormal density field was then used to create a catalogue that matches the luminosity-dependent clustering of the 2dFGRS sample. To facilitate this process we made a number of simplifications. First, we used the same grid both to create the catalogue and to estimate the power spectrum. There was therefore no need to create a full catalogue; instead, we can determine a catalogue already sampled on the grid. The additive nature of the Poisson distribution meant that the total number of galaxies at each grid point could be calculated by drawing a random Poisson variable with mean given by the selection function multiplied by the lognormal field and the mean expected bias at that grid point. These galaxies then need to be assigned luminosities. As we simply wish to use the mock catalogues to test the analysis method, we choose to only model the net effect, which is that the effective bias at a survey location depends on the distance from the observer. We therefore assume that the galaxies at each grid point all have the same luminosity, given by the average luminosity of the 2dFGRS sample at that distance, and that they have the same average expected bias. This approach can be interpreted as a special case where we are modeling power spectrum evolution along the line-of-sight rather than luminosity-dependent clustering.

We now describe how we calculated the biased lognormal density field. For the 2dFGRS sample of P01, the mean expected bias as a function of redshift is well fit by the formula

$$\langle b(r) \rangle = \int dL \bar{n}(\mathbf{r}, L) b(\mathbf{r}, L) = 0.85 + 6z^{1.75}, \quad (34)$$

where z is the redshift corresponding to a given radius.

There are a number of ways that one could apply this formula to create a biased density field. Perhaps the most rigorous method would be to create a number of lognormal fields with the same phases and different amplitudes, each corrected from the desired clustering strength as detailed above. We should then use the field corresponding to the desired power amplitude at each grid point. However, this would have been computationally very expensive. In the linear regime of interest, the fields are all of small amplitude and the correction between Gaussian and lognormal fields is very small. We therefore created a single lognormal field corresponding to the largest mean expected bias in the 2dFGRS sample $b(L) \sim 1.4b(L_*)$, and multiplied this field by the expected mean bias given by Eq. 34 divided by 1.4. By choosing to create the field for the largest mean bias we ensure that $\delta_{LN}(\mathbf{r}) > -1 \forall \mathbf{r}$. Alternatives would have been to bias either the Gaussian field $\delta_G \rightarrow b(L)\delta_G$, or to set $(1 + \delta_{LN}) \rightarrow (1 + \delta_{LN})^{b(L)}$. This choice is not signif-

icant, and all options result in fields with $\delta_{LN}(\mathbf{r}) > -1 \forall \mathbf{r}$, and approximately the correct varying clustering strength.

3.3 Analysis of mock catalogues

In order to test our derivation of optimal weights, we consider three weighting schemes. First we consider the weights derived to be optimal for a narrow k -space window

$$w_1 = \frac{b^2(\mathbf{r}, L)P(k)}{1 + \int dL \bar{n}(\mathbf{r}, L)b^2(\mathbf{r}, L)P(k)}. \quad (35)$$

The second weighting scheme that we consider is designed to highlight how luminosity-dependent bias affects the results of P01, and is given by

$$w_2 = \frac{b(\mathbf{r}, L)P(k)}{1 + \int dL \bar{n}(\mathbf{r}, L)b^2(\mathbf{r}, L)P(k)}. \quad (36)$$

The $b(\mathbf{r}, L)$ term in the numerator cancels the $1/b(\mathbf{r}, L)$ factor in Eq. 6 applied to each galaxy to correct the differing clustering strengths. Using these weights is therefore equivalent to the original FKP scheme, except that there is an additional $b^2(\mathbf{r}, L)$ in the denominator. This form was chosen rather than the exact FKP weight because this additional term is simply equivalent to varying $P(k)$ as a function of \mathbf{r} , and keeping the denominator fixed for all three weights enables the effect of the bias term in the numerator to be more easily understood.

In addition we consider weights that apply no distinction between galaxies with different expected biases

$$w_3 = \frac{P(k)}{1 + \int dL \bar{n}(\mathbf{r}, L)b^2(\mathbf{r}, L)P(k)}. \quad (37)$$

For the analysis presented in the next Section, we assumed a fixed value of $P(k) = 5000 h^3 \text{Mpc}^{-3}$ for all of the weighting schemes. The squared window functions $|G(\mathbf{k})|^2$ were calculated as in Eq. 15, and were spherically averaged as for the power estimate (Eq. 17). The data were then fitted with a smooth curve calculated using a Spline3 algorithm (Press et al. 1992). This curve was found to be a better fit to the shape of the recovered window at $k > 0.1 h \text{Mpc}^{-1}$ than the fitting formula of P01. For $k > 0.6 h \text{Mpc}^{-1}$, we extrapolate the window function as k^{-4} . This extrapolation does not significantly affect the shape of the recovered convolved power, although it does have a slight effect on the normalization.

As we have shown in Eqns. 6 & 15, although the galaxies were multiplied by the weight divided by the expected bias, the window function is only dependent on the weight. In an FKP analysis, such as P01, the weight assumed for the window function is the same as the multiplicative factor in Eq. 6, $w(\mathbf{r}, L)/b(\mathbf{r}, L)$. For example, if weights w_2 were applied to the galaxies in an FKP analysis of a catalogue with luminosity dependent clustering, weights w_3 would be assumed for the window function. Similarly, if weights w_1 were applied to the galaxies, weights w_2 would be assumed for the window function. Because we fix $P(k)$ in these weights as in P01, then the change in the shape of the recovered power spectrum is only dependent on this change in the window (see Section 2.1). The importance of the changing window on the shape of the power spectrum is considered in the next Section where we present the recovered power spectra from our mock catalogues calculated using weights w_1 , w_2 , and w_3 .

Because we create the mock catalogues and power estimates on the same grid, we know the selection function at each grid point

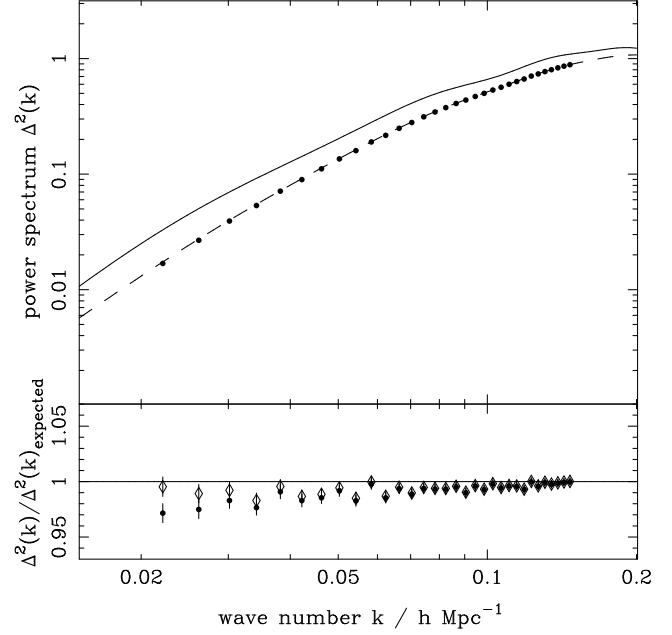


Figure 1. Top panel: the average recovered power spectrum from 1000 mock catalogues calculated within a selection function designed to mimic the 2dFGRS sample analysed by P01 (solid circles). These data were weighted using weights w_1 given by Eq. 35. For comparison we also plot the input power spectrum (solid line) and the power spectrum convolved with the fit to the spherically averaged Fourier window function (dashed line). In the lower panel, these data are compared with the models in more detail, and we plot the ratio of the average recovered power to the convolved model (solid circles with 1σ errors). The open diamonds show the ratio of the data to the expected convolved power including correction for the self-normalization induced by matching the average galaxy density (see Section 2.4 for details).

exactly. We can therefore easily subtract the mean galaxy density without having to create a synthetic catalogue. In order to determine the shot-noise level and the power normalization we require two integrals, given by Eqns. 16 & 7 respectively. As we are assuming that the distribution of galaxy luminosities is a delta function at each grid point, and we know the selection function at these points, then it is relatively straightforward to calculate these two quantities by numerically integrating over the grid used. In the following we apply the method described in Section 2.1 to estimate the power at 100 points evenly spaced in $0 < k < 0.128\pi h \text{Mpc}^{-1}$. This sampling is matched to that of P01.

3.4 Results

We have created 1000 lognormal catalogues as described in Section 3.3, and have analysed these catalogues using the three different weighting schemes given in Section 3.3. In this paper we only consider the recovered power for $0.02 < k < 0.15 h \text{Mpc}^{-1}$. This matches the region considered in P01 and avoids the non-linear regime $k > 0.15 h \text{Mpc}^{-1}$, where the Gaussian behaviour of the lognormal catalogues is expected to break down. In fact we do find a turn-up of the data for $k > 0.15 h \text{Mpc}^{-1}$, consistent with the non-linear behaviour of the lognormal model. The top panel of Fig. 1 shows the average recovered power spectrum for $0.02 < k < 0.15 h \text{Mpc}^{-1}$, calculated from the mock catalogues weighted with weights w_1 (solid circles) compared to the power expected from fitting to the radially averaged Fourier window func-

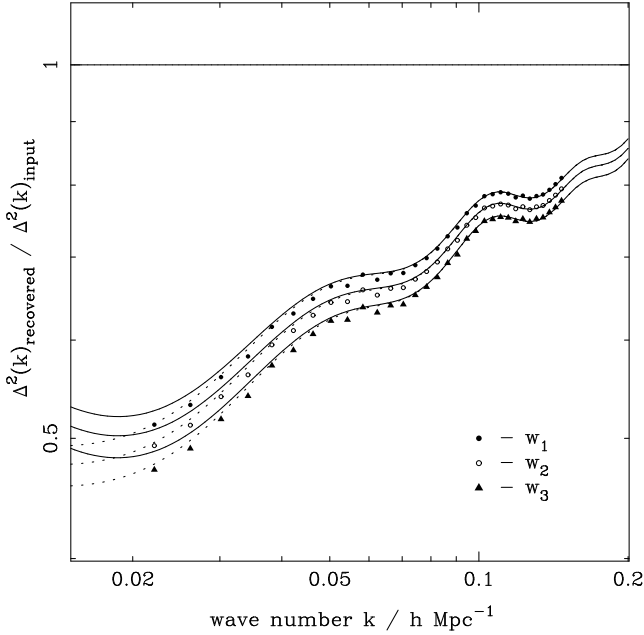


Figure 2. The average recovered power spectrum from 1000 mock catalogues, weighted as given by Eqns. 35 to 37, ratioed to the input power (symbols). These data are compared with the expected power calculated by convolving a fit to the spherically averaged Fourier window function with the input power (solid lines). The dotted lines include the correction for the self-normalization induced by matching the average galaxy density (see Section 2.4 for details).

tion for weighting scheme w_1 (dashed line); the solid line is the input power spectrum (not convolved with the window).

In order to examine the fit in detail and compare the average recovered power from the three weighting schemes, we ratio this power to the input power spectrum in Fig. 2. Here we see that the increasing factor of bias in the weights $w_3 \rightarrow w_1$ increases the effective size of the window in real space, and therefore reduces the effect of the window in Fourier space: weighting scheme w_1 produces the largest real-space volume as it increases the importance of the rare high-luminosity galaxies at high redshift the most.

The recovered diagonal elements of the covariance matrix calculated using the three weighting schemes were very similar in amplitude, so the number of realizations analysed was insufficient to distinguish the relative errors in the recovered power produced by the different the weighting schemes using this statistic. However, the smaller k -space window function created using weights w_1 does mean that this scheme is better at finding features in the power spectrum compared with the other weighting schemes.

The difference between the convolved power for w_2 and w_3 corresponds to the small offset induced by not correcting for luminosity-dependent clustering. This is illustrated in Fig. 3, where the open circles show the ratio of the average power spectrum recovered from the mock catalogues using the original FKP method (calculated using weights w_2 , Eq. 36) with the expected power (the input power spectrum convolved with the window function corresponding to weight w_2). The solid line show the expected ratio of 1. The errors on the data are dominated by cosmic variance and are given by the square root of the diagonal elements of the covariance matrix. The solid squares with one sigma errors show the ratio of the the same recovered power spectrum with the matter power spectrum convolved with the window relative to weights w_3 ,

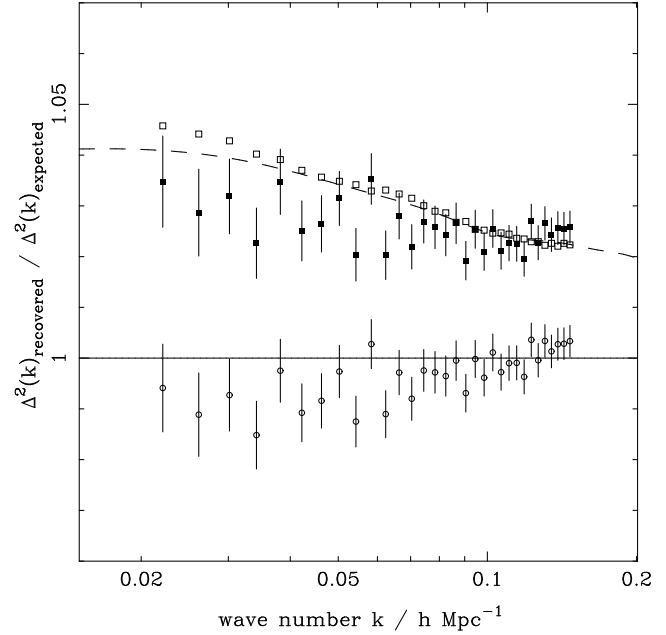


Figure 3. The average recovered power from the mock catalogues, calculated using weight w_2 given by Eq. 36 ratioed to the expected power (open circles with 1σ errors). The solid line shows the expected ratio of 1. The solid squares with 1σ errors show the same average recovered data, compared to the model convolved with the window calculated from weights w_3 , those assumed in the standard FKP analysis. The dashed line shows the expected ratio in this case. The errors on the data are dominated by cosmic variance: ratioing the two recovered average power spectra for the two weights gives the open squares. We see that not allowing for luminosity-dependent clustering, equivalent to assuming the wrong window, changes the power spectrum normalization and induces a slight change of slope.

the window assumed without correcting for luminosity-dependent clustering. The dashed line shows the expected ratio. In the next section we consider how this offset affects the 2dFGRS analysis of P01.

4 APPLICATION TO 2DFGRS ANALYSIS OF P01

In the analysis of P01, no correction was made for the varying bias caused by the range in galaxy luminosities within the sample. As described in Section 2.1, this causes the incorrect window function to be assigned to the analysis. In the top panel of Fig. 4 we compare the recovered 2dFGRS power spectrum data with a model power spectrum convolved with both the window function calculated using the FKP method, and that calculated after correction for luminosity dependent bias (calculated with weights given by $b(L)w(r)$, see Section 2.1). The corrected window function has a smaller effect on the power compared with the original because the extra bias weighting increases the effective size of the survey. The models in this figure vary slightly from those presented and used by P01, as we have fitted the spherically averaged window functions using Spline3 fits as described in Section 3.3. Changing how each spherically averaged window was fitted has very little effect on the shape of the recovered convolved power spectra, but it can affect the normalization ($\sim 10\%$), depending on the exact nature of the fits. This will be discussed further in a subsequent paper.

The effect of not assuming the correct window when fitting the recovered power spectrum slope and amplitude of the 2dFGRS

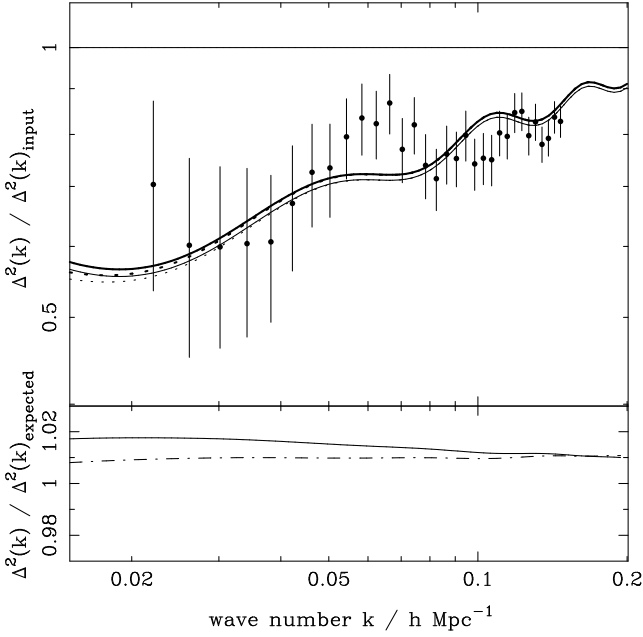


Figure 4. Top panel: the 2dFGRS power spectrum data of P01 (solid points) with errors given by root of the diagonal elements of the covariance matrix. These data are compared with the concordance model ($\Omega_m = 0.3$, $\Omega_b/\Omega_m = 0.15$, $\Omega_\Lambda = 0.7$, $h = 0.7$, $n_s = 1$) power spectrum convolved with the window function used in P01 (lower thin solid line), and with the corrected window function allowing for luminosity-dependent bias (upper thick solid line). In this plot, the 2dFGRS data have been fitted to the upper thick solid line. The dotted lines include the correction for the self-normalization of the galaxy number density. All of the data are ratioed to the unconvolved concordance model power spectrum. The difference between the two convolved models is negligible compared to the errors in the 2dFGRS power. The ratio between the two convolved models gives the effect of not correcting for luminosity-dependent bias, and is plotted in the lower panel of this Figure (solid line). The change in shape induced is closely matched by a change in the spectral index of the fitted model – the dot-dash line shows the ratio of a convolved power spectrum with $n = 1$ and the window function allowing for luminosity dependent bias divided by a power spectrum with $n = 0.995$ and a window function as assumed in a FKP analysis: the shape of the power spectrum recovered in a universe with $n = 1$ would be fitted by a power spectrum with $n = 0.995$ convolved with the original FKP window.

analysis of P01 is quantified in the lower panel of Fig. 4. The solid line is the ratio of the expected power spectrum from a sample of galaxies with luminosity-dependent bias within a concordance universe ratioed to a theory power spectrum with the same cosmological parameters but with $n = 0.995$ instead of $n = 1$, convolved with window assumed in P01. This small shift in n is sufficient to correct the change in shape caused by assuming the wrong window, and is approximately equivalent to a change $\Delta\Omega_m h \simeq 0.0014$. This change is obviously very small compared with the statistical errors on the recovered parameters. There is also a small systematic error on the power spectrum amplitude of $\lesssim 2\%$, reflecting the change in the normalization of the spherically averaged windows. The solid line in the lower panel of Fig. 4 is comparable with the dashed line in Fig. 3, which shows the same effect for the mock catalogues. The difference between the two lines is caused by the change in the denominator of Eqns. 36 & 37, compared with the original FKP weightings. The extra factor of $b^2(r, L)$ in Eqns. 36 & 37 decreases the importance of the high redshift data, so the factor of $b(r, L)$ on the numerator has more effect.

Using the revised window when fitting to the published 2dFGRS power spectrum data of P01 changes the recovered $\Omega_m h$ and Ω_b/Ω_m values very slightly (to higher $\Omega_m h$ and lower baryon fraction), but gives best-fit parameters $\Omega_m h = 0.20 \pm 0.03$ and $\Omega_b/\Omega_m = 0.15 \pm 0.07$ (68% confidence interval, assuming $n_s = 1$ & $h = 0.7 \pm 0.07$), that are the same as those reported by P01 at this significance.

5 DISCUSSION

We have presented a method for the Fourier analysis of galaxy redshift surveys that allows for luminosity-dependent clustering. Although this generalization of the FKP analysis method is specifically designed to allow for luminosity-dependent clustering, the derivation is actually more general and can be applied to any mixed distribution of galaxies with differing clustering strength. Consequently, it can cope with type-dependent clustering, power spectrum evolution and bias evolution, and should therefore be of use in the analysis of future deeper redshift surveys. The method requires knowledge of the relative change in the bias as a function of galaxy properties, although to recover the matter power spectrum amplitude, the absolute bias is required.

The optimal weights presented in this paper (Eq. 28) differ from those of Yamamoto (2003), ignoring the correction for redshift-space distortions (equation 29 of Yamamoto 2003). This results from the fact that we included the effect of luminosity-dependent clustering at the inception of our optimal weight derivation and minimized the error in the underlying matter power spectrum. Yamamoto (2003) instead minimized the error in the galaxy power spectrum (biased power in the language of this paper). Consequently in our weighting scheme, luminous galaxies are given a higher weight than less luminous galaxies: they contribute more signal-to-noise to the measure of the underlying fluctuations than less luminous galaxies. However, this is not true if we wished to optimize for the biased power as shown by Yamamoto (2003). The weighting scheme that should be adopted depends on the statistic to be measured: if we wish to measure the underlying matter power spectrum, then the weights derived in Section 2.3 are more applicable.

The derivation of optimal weights was performed in the limit of a negligible window function. On scales comparable to the size of the window, the optimal weights will change, and will depend on the survey geometry such that the weights no longer have radial symmetry (e.g. Hamilton 1997). Although the three radially symmetric weighting schemes considered in Section 3.3 differed by a factor of ~ 2 over the redshift range of interest, they resulted in remarkably similar diagonal errors in the power spectrum. If we constrain the weights to be radially symmetric then small deviations away from the derived optimal distribution do not appear to have a significant effect on the recovered errors.

For P01, the error induced by not allowing for the effect of luminosity-dependent clustering was shown to be negligible in Section 4. One of the factors that contributed to this was that, in the weights applied, $P(k)$ was fixed at $P(k) = 5000 h^3 \text{Mpc}^{-3}$. This was not the case in many other Fourier analyses of galaxy redshift surveys (e.g. Tegmark, Hamilton & Xu 2002) which use a weight that varies as a function of k . Varying the estimated power used in Eq. 28 changes the normalization N (Eq. 7), which works in conjunction with the change in shape of the spherically averaged window to alter the recovered power. As we have shown in this paper,

it is possible to correct these effects by using the correct window function at each k -value.

Redshift space distortions caused by peculiar velocities will also affect the shape of the recovered power spectrum. In the spirit of generalizing FKP, such effects are not included here. However P01 used mock catalogues drawn from the Hubble volume simulation to show that these were not significant on the scales ($0.02 < k < 0.15 h \text{ Mpc}^{-1}$) considered in this work. This issue will be explored further in a later paper.

6 ACKNOWLEDGMENTS

We thank Peder Norberg and Max Tegmark for stimulating discussions. WJP is supported by PPARC through a Postdoctoral Fellowship. LV is supported by NASA through Chandra Fellowship PF2-30022 issued by the Chandra X-ray Observatory Center, which is operated by the Smithsonian Astrophysical Observatory on behalf of NASA under contract NAS8-39073. JAP is grateful for the support of a PPARC Senior Research Fellowship. WJP and LV would like to thank the Aspen Center for Physics where the initial stages of this work were carried out during the ‘‘Structure Formation in the Era of Large Surveys’’ workshop, June 2002.

REFERENCES

- Bennett C.L., et al. (WMAP consortium), 2003, ApJ submitted, astro-ph/0302207
- Benson A.J., Cole S., Frenk C.S., Baugh C.M., Lacey C.G., 2000, MNRAS, 311, 793
- Coles P., Jones B., 1991, MNRAS, 248, 1
- Colless M., et al., 2001, MNRAS, 328, 1039
- Davis M., Geller M.J., 1976, ApJ, 208, 13
- Dekel A., Lahav O., 1999, ApJ, 520, 24
- Efstathiou G., et al. (2dFGRS consortium), 2002, MNRAS, 330, 29
- Eisenstein D.J., Hu W., 1998, ApJ, 496, 605
- Feldman H.A., Kaiser N., Peacock J.A., FKP, 1994, ApJ, 426, 23
- Hamilton A.J.S., 1997, MNRAS, 289, 285
- Hamilton A.J.S., 1998, in ‘‘The evolving Universe’’, Astrophysics and space science library Series, 231, 185
- Hawkins E., et al. (2dFGRS consortium), 2003, MNRAS accepted, astro-ph/0212375
- Hinshaw G., et al. (WMAP consortium), 2003, ApJ submitted, astro-ph/0302222
- Lahav O., et al. (2dFGRS consortium), 2002, MNRAS, 333, 961
- Norberg P., et al. (2dFGRS consortium), 2001, MNRAS, 328, 64
- Norberg P., et al. (2dFGRS consortium), 2002, MNRAS, 332, 827
- Peacock J.A., Nicholson D., 1991, MNRAS, 253, 307
- Peacock J.A., Dodds S.J., 1994, MNRAS, 267, 1020
- Peacock J.A., et al. (2dFGRS consortium), 2001, Nature, 410, 169
- Peebles P.J.E., 1980, The large-scale structure of the universe. Princeton University Press
- Percival W.J., et al. (2dFGRS consortium), P01, 2001, MNRAS, 327, 1297
- Percival W.J., et al. (2dFGRS consortium), 2002, MNRAS, 337, 1068
- Press W.H., Teukolsky S.A., Vetterling W.T., Flannery B.P., 1992, Numerical recipes in C, 2nd ed. Cambridge Univ. Press
- Seaborne M., et al., 1999, MNRAS, 309, 89
- Smith R.E., et al. (Virgo consortium), 2002, MNRAS submitted [astro-ph/0207664]
- Spergel D.N., et al. (WMAP consortium), 2003, ApJ submitted, astro-ph/0302209
- Tadros H., Efstathiou G., 1995, MNRAS, 276, L45
- Tegmark M., Hamilton A.J.S., Xu Y., 2002, MNRAS, 335, 887
- Tegmark M., et al. (SDSS consortium), 2003, ApJ submitted
- Verde L., et al. (2dFGRS consortium), 2002, MNRAS, 335, 432

Verde L., et al. (WMAP consortium), 2003, ApJ submitted, astro-ph/0302218

Yamamoto K., 2003, ApJ accepted, astro-ph/0208139

York D.G., et al. (SDSS consortium), 2000, AJ, 120, 1579

Zehavi I., et al. (SDSS consortium), 2002, ApJ, 571, 172